EXPERIMENTAL-NUMERICAL RESISTIVITY MEASUREMENTS APPROACH FOR CHARACTERIZATION IN STRUCTURAL TIMBER

Pham Minh Dung, Tuan Anh Nguyen, Wael Hafsa, Nicola Angellier, Laurent Ulmet, Mokhfi Takarli, Octavian Ion Pop, Frédéric Dubois

EXPERIMENTAL-NUMERICAL RESISTIVITY MEASUREMENTS APPROACH FOR CHARACTERIZATION IN STRUCTURAL TIMBER

Pham Minh Dung[1], Nguyen Tuan Anh[2], Hafsa Wael[3], Angellier Nicola[4], Ulmet Laurent[5], Takarli Mokhfi[6], Pop Ion Octavian[7], Dubois Frédéric[8]
[1]GC2D, University of Limoges, 19300, Egletons, France, minh-dung.pham@etu.unilim.fr;
[2]Ho Chi Minh City University of Transport, tuananh.nguyen@ut.edu.vn

***Abstract**: This paper deals with an experimental and numerical approach to adapt resistivity measurements, usually developed in geophysics, for the in-situ monitoring of moisture content in structural timber. This method leads to identifying timber resistivity fields, in relation to moisture content, by crosschecking the current lines injected by electrodes connected to the reachable surfaces of the investigated timber element. More precisely, it is composed of the inversion of a numerical model of electrical current injection implemented in a finite element software, through a method to minimize the error between simulation and measurements. For starters, the direct model reproduces the physical measurement: the current injection and potential difference measurement from an electrical quadrupole. Next, the inversion algorithm reconstructs the timber resistivity field from the measured resistivity data.*

***Keywords**: Timber, inverse method, resistivity.*

***Classification number:** 2.4*

1. Introduction

Moisture content control is currently carried out only occasionally during the manufacturing of timber components or on in-situ timber elements using surface and point measurement techniques [1; 4; 7; 12]. However, by taking sports complex frames or bridges as an example [5; 6], the cross-sections of elements necessitate a controlling moisture into the section during the structure life. For this reason, the time measurement of moisture in the cross-sections is key to structural durability when monitoring the actual condition of timber elements.

In this context, the present work focuses on the development of a non-destructive diagnostic tool to obtain a representative distribution of moisture in the cross-section overlapping innovative and numerical approaches for in-situ laboratory applications. Improved three-dimensional resistive methods should provide a response to this issue by linking overall wood resistivity with moisture content level. However, this technique which is typically used in geophysical applications [8] requires a calibration protocol to output the moisture-resistivity transfer curves [11]. For this purpose, the moisture content profile definition at the laboratory scale has been proposed by Nguyen & al. [10] with the use of gamma densitometry technique to determine the moisture content concentration [3]. The first section provides the current injection protocol using a four-quadrupole configuration resistivity-meter coupled to a multiplexing system, which yields the resistance measurement for each quadrupole.

The finite element implementation of Ohm's law, in deriving the simulation of the measurements, is developed in the second section. The probe mesh is uniquely focused and a specific algorithm enables reproducing the multiplexing process.

The third part deals with the inverse method, resulting in an optimization of the numerical resistivity field to minimize errors between experimental and calculated resistivity along all multiplexing sequences. An experimental application supplements theoretical developments.

2. Experimental tools for the electrical current injection

The resistivity-meter used is a Syscal Junior Switch 48 from Iris Instruments, i.e. the combination of a multiplexing system (up to

48 electrodes) and a power supply (100 W). The principle here is to transmit a current of intensity I between two injection electrodes (C1 and C2) and measure the difference in potential V between the other two (P1 and P2) to obtain a resistivity mapping, figure 1.

Since the resistivity-meter had originally been developed for geophysical applications, it is necessary to control its adaptability to timber material, which covers other resistivity ranges as well. Specific cables and miniaturized electrodes were therefore designed. Furthermore, a power divider module was added to increase the current injection range, Figure 1. In this case, the maximum intensity of injected current provides a usable measurement of difference in potential of high resistivity values. The resolution range thus extends from $1.e^{-3}$ m·A to $2.e^{-4}$ m·A.

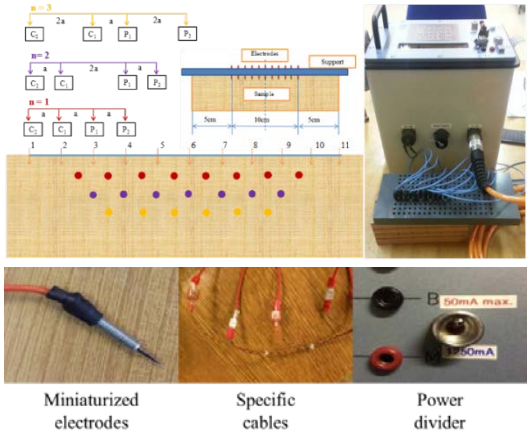

Figure 1. *Distribution of electrodes and 3 dipole-dipole levels.*

So, the device developed is suitable for average moisture contents down to 13 %. This limit should be lowered by improving the quality of the contact between timber and electrodes, for example by increasing their penetration depth.

The studied configuration relates to a belted two-dimensional measurement for homogeneous moisture content. This choice result of the expected accessible configuration in wooden structures concerned by moisture content penetration: in the span middle, the diffusion is characterized by a radial transverse mass transfer in accordance with this two-dimensional scenario.

A cubic sample 95 x 95 x 95 mm^3 in dimension is machined on a Douglas fir volume. The sample is placed in a desiccator, with a constant humidity of 86 %HR. The experimental device is placed in a chamber in which the temperature is fixed to 20 °C.

As shown in Figure 2, before the hydric loading, the sample was belted with 20 electrodes: 5 electrodes on each side spaced 1.5 cm apart at depth of 1 cm.

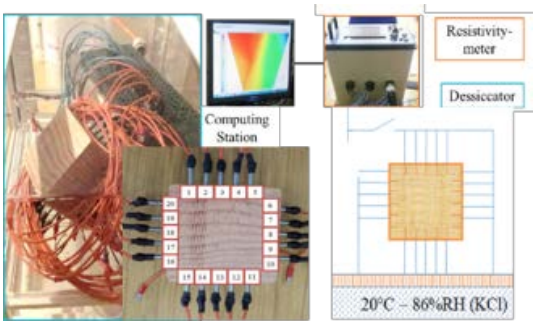

Figure 2. *Layout and numbering of electrodes.*

The experimental device developed was ultimately composed of the modified resistivity-meter connected to the computing station for the data acquisition and the conditioning desiccator. This latter had also been modified to insert the resistivity-meter cables so as to avoid moving the samples during measurements which were conducted once equilibrium had been reached.

Most electrical measurements were performed twice by considering multiplexing with dipole-dipole configurations to complete the data identifying the resistivity field per an inversion method. Multiplexing 1 from electrode 1 to 20 and multiplexing 2 from electrode 11 to 10 were conducted, with all quadrupole configurations utilized to investigate the entire transverse section with a high density of measurement points, both at the surface and through the depth, for a total of 319 measurements for each multiplexing step. The observed values remain consistent with the expected moisture content once equilibrium has been achieved.

3. Direct numerical models for the electrical current injection

The finite element software Castem ([2]) has been employed for the simulation of the multiplexed measurements by combining an

Ohm's Law resolution (current injection and potential calculus):

$$\vec{J} = -\sigma\overrightarrow{grad}(V) \quad (1)$$

The meshing step of the finite element model must initially define the discretization of electrodes placed for both the current injection and potential measurement locations and then the discretization of the sample volume. Although this study is limited to 2D diffusion problems, the current injection also imposes a spatial discretization. However, the symmetry of the studied configurations makes it possible to discretize just half-samples. Electrodes are semi-cylinders with a radius of 1 mm and length of 1 cm delivering a current density forced onto the electrode surface, extending to the contact surface between electrodes and wood sample; the wood in the vicinity of the electrode is a volume, appended to the rest of the sample, for which an electrode installation area has been preserved. As shown in Figure 3, the mesh size gradually increases, until the sample size has been reached, in order to facilitate the resolution.

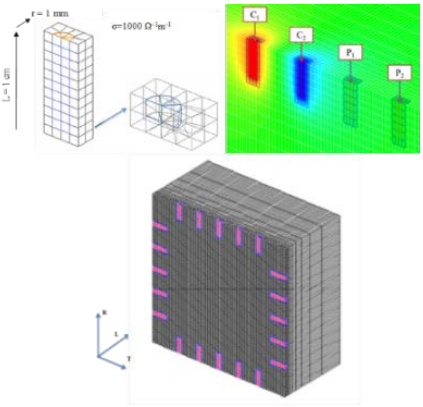

Figure 3. *Meshing of an electrode and surrounding wood volume, and the meshing of half-samples and numerical current injection.*

The last step consists of placing the electrodes on the samples at a spacing of 1.5 cm. Let's note that electrodes are considered to be perfectly conductive. In accordance with a linear Ohm's Law, the resistance value remains independent of potential or injected current: the model injects current with an intensity of 1 A.

The purpose of the measurements is to determine the distribution of resistivity inthe transverse section of the sample (hypothesis of constant resistivity in the longitudinal direction). Since resistivity trends exponentially with respect to moisture content ([11]), we have explored the case of an exponential resistivity gradient (to simulate a linear moisture content gradient) in tangential direction by discretizing the sample with a large mesh (made up of 5 x 5 elements. Each element is assigned a homogeneous resistivity value, Figure 4. To solve the direct model, the coarse-meshed resistivity field is firstly projected into the fine mesh including electrodes. In a second step, the simulation calculates the electrical resistance via the various multiplexing steps.

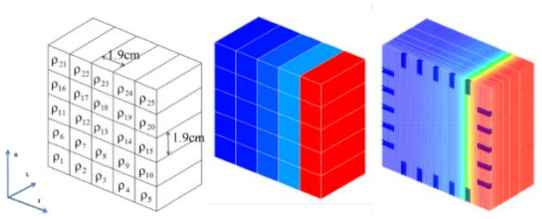

Figure 4. *Discretization of sample, resistivity field projection.*

The direct model resolution, with multiplexing 1 and 2, considers 319 simulated measurement points. As expected, the calculated resistance values evolve exponentially between the dry face and the wet face while remaining constant on the two faces. Moreover, in both cases, the direct model can numerically simulate the electrical resistance measurement with multiplexing.

4. Inverse identification method applied to resistivity fields

The numerical inversion strategy relies on developing an inverse method implemented with the Castem software to model and estimate the real resistivity field in studied finite volume samples. M electrical conductivity $m_i=(1,2,\ldots,M)$ need to be identified. The investigated medium is discretized by a grid (coarse meshing) with constant conductivity in each cell, as represented by a vector $m=(m_1,m_2,\ldots,m_M)$ used to deduce resistivity such as:

$$m_{resistivity} = \left(\frac{1}{m_1}, \frac{1}{m_2}, \ldots, \frac{1}{m_M}\right) \quad (2)$$

The measured resistances are considered as a data vector $d=(d_1,d_2,\ldots,d_N)$, with N

depending on the multiplexing. The direct problem is then defined as a function f(m) , whose result is a vector compound of calculated resistances from the direct model. The resolution of an inverse problem calls for optimizing model parameters in order to minimize the difference between measured and calculated data, yielding to the following objective function:

$$F = (\Delta d - J\Delta m)^T.(\Delta d - J\Delta m) \quad (3)$$

$\Delta d=d-f(m_0)$ is the difference between measured and calculated data.

This inversion model relies on the Levenberg-Marquadt algorithm [9], i.e. according to the following expression:

$$\Delta m = (J^T J + \lambda W_m)^{-1} J^T \Delta d \quad (4)$$

W_m is an MxM identity matrix.

This model includes a damping factor λ that allows for convergence to a realistic solution, which is used dynamically: the first iteration is performed with a high enough value ($1e^{16}$) compared to the high terms of the Jacobian matrix J. The stop criterion f_m , set at $1e^{-3}$, is based on the parameters variation between two successive iterations:

$$\left|\frac{m_{i+1} - m_i}{m_i}\right| \le f_m \quad (5)$$

The validation of the inversion algorithm uses data resolved by the direct model and injected into the inverse model as measured data, with knowledge of the real resistivity field allowing for model validation. The known resistivity field is the exponential gradient between $1.e^4$ and $1.e^6$ Ω·m in the tangential direction for the sample, Figure 4. The numerical resistance values are used as "measured" data. The initial solution, i.e. a constant resistivity field with $\rho=1.e^7$ Ω·m, has been selected sufficiently far from the desired solutions. The sample is discretized with cells, each of which assigned constant resistivity values that are assumed to be the unknowns to identify.

Each iteration lasts 1 hour and convergence requires 12 iterations. The estimated result exhibits an average error of 0.5% on "measured" resistances $|\Delta V_{P1P2}/I_{C1C2}|$, ultimately leading to a maximum error of 6% between estimated and real resistivity, Figure 5. So, identification difficulties are concentrated in the middle of the sample.

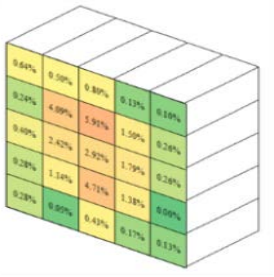

Figure 5: *Errors between "real" and estimated resistances and resistivities*

This example shows that the inversion algorithm, in combining "simulated" and modeled experimental measurements, leads to encouraging results. This validation must now be completed with some truly experimental applications.

We now focus on the application of the inversion model to determine resistivity in the sample from the experimental measurements. Regardless of the inversion algorithm, results directly depend on the ability of the resistivity-meter to record measurements on long current lines in a highly resistive medium. By comparing the shared quadrupoles of each multiplexing, it is observed that the quadrupoles including some electrodes do not yield the same or consistent values, prompting us to suspect either an injection problem for these electrodes or aberrant potential measurements (current lines too long, resistivity too high). This observation mainly underscores the decrease in workable measurements for the identification algorithm, and consequently the need to adapt the discretization grid to its particular use, Figure 6.

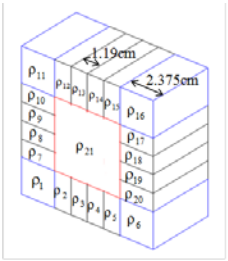

Figure 6: *The new discretization grid for the 2D sample.*

Once again, a constant resistivity field ($\rho=1e^7$ Ω.m) has been chosen as the initial field at the beginning of the inversion process. A comparison of measured and identified resistances for three different discretization grids is shown:

- 25 cells (5 x 5) used during the numerical validation step: the algorithm does not converge, as the 25 selected resistivity values are heterogeneous (i.e. the ratio between maximum and minimum values exceeds 1000);

- 9 cells (3 x 3): The algorithm converges after 14 iterations, with the 9 identified resistivity values being homogeneous (ratio between maximum and minimum values equal to 25);

- 21 cells: The algorithm converges, the 21 identified resistivity values are relatively homogeneous (ratio between maximum and minimum values stands at 50), figure 7.

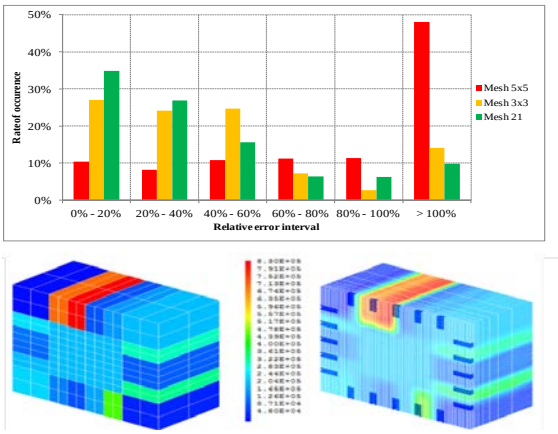

Figure 7. *Error occurrence between simulated and measured resistances and inversion results (resistivity in Ω·m).*

This ultimately shows that the choice of newly proposed grid in figure 6 is better adapted to missing experimental data and clearly decreases the error. As a result, in figure 7, we have more confidence in the estimation of resistivity values with this configuration.

Resistivity identification remains unsatisfactory at this study stage, especially for an approach that includes monitoring. The proposed method is a priori not subject to questions since it reveals good performance across simulations. Difficulties appear to focus on the experimental machinery, which could be upgraded to decrease current line length or else increase the resistivity range measurement. The authorized power of the equipment prevents conducting in-depth measurements inside the samples. The large number of unworkable measurements leads to a data shortage for the numerical inversion convergence with low error.

5. Conclusion and perspectives

In this work, a new experimental and numerical strategy for monitoring timber structures has been proposed. In the aim of a moisture content measurement with electrical tomography, we have presented the entire set of tools developed, leading to an experimental protocol capable of determining the resistivity field in timber elements by coupling a multiplexed resistivity measurement with a numerical inversion.

This device is numerically validated and we have displayed the first experimental applications. The measurement difficulties encountered stemmed from the studied material (high resistivity values), its geometry (long current lines) and the resistivity-meter itself (current injection limitation).

The 2D approach is focused on the determination of the moisture content fields in a transverse section. While this case is more attractive for structural monitoring, we encountered the physical limitations of measurement material employed: these difficulties were tied, on the one hand, to high resistivity over depth (dry zones) and long current lines, and on the other hand to a resistivity-meter adapted to geophysical measurements and not to such a resistive material like timber. The tool needs to be improved in this aspect because the level of precision obtained is not satisfactory for the anticipated monitoring approach.

In the short run, improving the experimental protocol will be considered along two main lines: 1) studying the effects of electrode type, number and location, 2) testing other quadrupole configurations (traversing, equatorial). A sensitivity study must be carried out in order to further the compromise between measurement precision,

depth measurement and the measured moisture content range. Varying the electrode lengths to collect information both on the surface and in depth can be considered even though the surface information will always be more reliable since in a timber structure, the moisture content profiles stems from the surface. In the long run, it is also envisaged to replace the resistivity-meter and compensate for the lack of measurements by numerically simulating the diffusion process. The present method can be used to define moisture content around the section edges with a good fit of external exchanges with humid air and wood permeability. A heat and mass transfer subroutine will serve to calculate moisture content at the section core. Today, the main obstacle consists of establishing the correlation between experimental and simulated region❑

Acknowledgements

The authors wish to strongly acknowledge the civil engineering university association (AUGC, http://www.augc.asso.fr/) for its financial support in the participation to this conference.

References

[1] Carll C., Ten Wolde A., (1996). Accuracy of wood resistance sensors for measurement of humidity. Journal of Testing and Evaluation, JTEVA, 24(3), 154–160.

[2] Cast3m, (2012), a research FEM environment; its development is sponsored by the French Atomic Energy Commission.

[3] <http://www-cast3m.cea.fr/>

[4] Da Rocha M.C., Da Silva L.M., Appoloni C.R., Portezan Filho O., Lopes F., Melquiades F.L., et al., (2001). Moisture profile measurements of concrete samples in vertical water flow by gamma ray transmission method. Radiat Phys Chem, 61(3-6):567-9.

[5] Dietsch P., Franke S., Franke B., Gamper A. (2014a) Methods to determine wood moisture content and their applicability in monitoring concepts, J. Civil Struct. Health Monit., 5 (2), pp. 115–127.

[6] Dietsch P., Gamper A., Merk M., Winter S. (2014b), Monitoring building climate and timber moisture

[7] Dubois F., Petit C., Sauvat N., Peuchot B., Cremona C., Fournely E., (2004). A Study about the mechanic behaviour of the timber bridge of Merle. 8th Word Conference on Timber Engineering WCTE2004, June 14-17 Lahti.

[8] Forsén H., Tarvainen V., (2000). Accuracy and functionality of hand held wood moisture content meters. VTT publications, 420, 95.

[9] Loke M.H. and Barker R.D., (1996). Practical techniques for 3D resistivity surveys and data inversion. Geophysical Prospecting, 44, 499-524.

[10] Marquardt, W., (1963). An algorithm for Least-Squares Estimation of Nonlinear Parameters. Journal of the Society for Industrial and Applied Mathematics, 11(2), 431–441.

[11] Nguyen T.A., Angellier N., Caré S., Ulmet L., Dubois F, (2017). Numerical and experimental approaches to characterize the mass transfer process in wood elements. Wood Science and Technology, DOI :10.1007/s00226-017-0898-5.

[12] Stamn A. J., (1927). The electrical resistance of wood as a measure of its moisture content. Ind Eng Chem, 19(9) 1021-1025.

[13] Ueno K., Straube J., (2008). Laboratory calibration and field results of wood resistance humidity sensors. Best 1: Building for Energy Efficiency and Durability at the Crossroads. Minneapolis.

Ngày nhận bài: 28/2/2018
Ngày chuyển phản biện: 2/3/2018
Ngày hoàn thành sửa bài: 23/3/2018
Ngày chấp nhận đăng: 30/3/2018